X. Li
Research Assistant
Department of Mechanical Engineering,
Clemson University,
Clemson, SC 29634-0921
e-mail: xianchl@clemson.edu

J. L. Gaddis
Professor
Mem. ASME
Department of Mechanical Engineering,
Clemson University,
Clemson, SC 29634-0921
e-mail: leo.gaddis@ces.clemson.edu

T. Wang
Professor
Mem. ASME
Energy Conversion and Conservation Center,
University of New Orleans,
New Orleans, Louisiana 70148-2220
e-mail: twang@uno.edu

Modeling of Heat Transfer in a Mist/Steam Impinging Jet

The addition of mist to a flow of steam or gas offers enhanced cooling for many applications, including cooling of gas turbine blades. The enhancement mechanisms include effects of mixing of mist with the gas phase and effects of evaporation of the droplets. An impinging mist flow is attractive for study because the impact velocity is relatively high and predictable. Water droplets, less than 15 μm diameter and at concentrations below 10 percent, are considered. The heat transfer is assumed to be the superposition of three components: heat flow to the steam, heat flow to the dispersed mist, and heat flow to the impinging droplets. The latter is modeled as heat flow to a spherical cap for a time dependent on the droplet size, surface tension, impact velocity and surface temperature. The model is used to interpret experimental results for steam invested with water mist in a confined slot jet. The model results follow the experimental data closely.
[DOI: 10.1115/1.1409262]

Keywords: Augumentation, Droplet, Evaporation, Heat Transfer, Impingement, Modeling

Introduction

The addition of mist to a flow of steam or gas offers enhanced cooling for many applications, including cooling of gas turbine blades [1–3]. The mechanisms of heat transfer enhancement include effects of mist momentum on the gas phase and effects of evaporation of the droplets, both directly and via the gas. Increased specific heat and lower bulk temperature are also typical features of a mist flow. In a mist/steam jet impingement flow, the interaction of the droplets and the target wall becomes pronounced because of the relatively high impact velocity and well defined because the velocity is relatively predictable.

While single-phase jet impingement cooling has been studied extensively, few studies have been found on mist jet impingement. Goodyer and Waterston [1] considered mist/air impingement for turbine blade cooling at surface temperatures above 600°C. They suggested that the heat transfer was dominated by partial contact between the droplets and the target surface, during which the droplets vaporized at least partially. A vapor cushion and the elastic deformation of the droplets were responsible for rejecting the droplets. Addition of 6 percent water was found to improve the stagnation point heat transfer by 100 percent, diminishing away from the stagnation point. Droplet size was found to have little effect for 30 μm $< d_{32} <$ 200 μm.

Takagi and Ogasawara [4] studied mist/air heat and mass transfer in a vertical rectangular tube heated on one side. They identified wet-type heat transfer at relatively low temperatures and post-dryout type at higher temperatures. In the wet region the heat transfer coefficient increased with increased heat flux. In the post-dryout region the heat transfer coefficient increased with droplet concentration and flow velocity and with decreased droplet size. Mastanaiah and Ganic [5] confirmed that the heat transfer coefficient decreased with increased wall temperature.

Yoshida et al. [6] focused on the effect on turbulent structure with a suspension of 50 μm glass beads. In the impinging jet region, the gas velocity was found to decrease due to the rebound of beads, accompanied by an increase in the normal direction velocity fluctuations. In the wall-jet region the effect was slight. The Nusselt number was found to increase by a factor of 2.7 for mass flow ratios (solid/gas) of 0.8.

Guo et al. [2] studied the mist/steam flow and heat transfer in a straight tube under highly superheated wall temperatures. It was found that the heat transfer performance of steam could be significantly improved by adding mist into the main flow. An average enhancement of 100 percent with the highest local heat transfer enhancement of 200 percent was achieved with less than 5 percent mist. In an experimental study with a horizontal 180 deg tube bend Guo et al. [3] found both the outer wall and the inner wall of the test section exhibited a significant and similar heat transfer enhancement. The overall cooling enhancement of the mist/steam flow increased as the main steam flow increased, but decreased as the wall heat flux increased.

To explore the mechanism of mist heat transfer, interaction of droplets with the wall has been studied extensively. Wachters et al. [7] considered the impact of droplets about 60 μm impacting a heated surface in the range of 5 m/s. Impinging droplets could only maintain the spheroidal state with relatively high surface temperatures. The required temperature depended on thermal properties and roughness of the surface as well as the Weber number of the droplets. In the spheroidal state very low rates of heat flow were observed.

To obtain fundamental information concerning the heat transfer processes in spray cooling, Pederson [8] studied the dynamic behavior and heat transfer characteristics of individual water droplets impinging upon a heated surface. The droplet diameters ranged from 200 to 400 μm, and the approach velocities ranged from 2 to 8 m/s. The wall temperature ranged from saturation temperature to 1000°C. Photographs of the impingement process showed that even the small droplets studied broke up upon impingement at moderate approach velocities. The heat transfer data showed that approach velocity was the dominant variable affecting droplet heat transfer and that surface temperature had little effect on heat transfer in the non-wetting regime. The droplet deformation and break-up behavior for droplets 200 μm in diameter did not appear significantly different from that for larger droplets. He also found that, for any given parameters in the non-wetting regime, a minimum velocity could exist below which the droplets deformed consistently without break-up.

Contributed by the Heat Transfer Division for publication in the JOURNAL OF HEAT TRANSFER. Manuscript received by the Heat Transfer Division June 7, 2000; revision received April 23, 2001. Associate Editor: V. P. Carey.

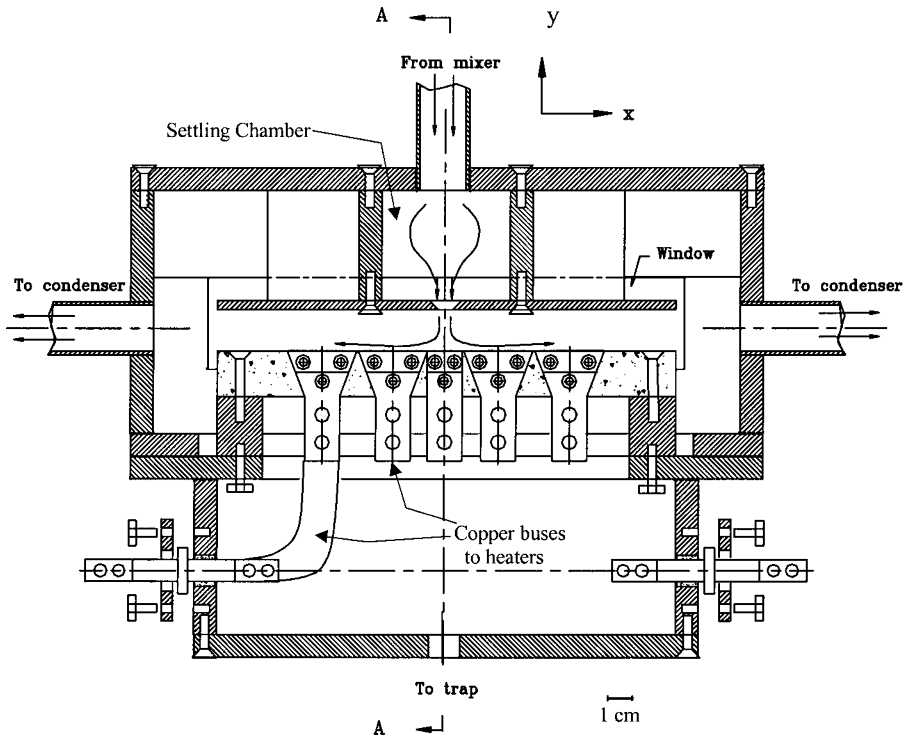

Fig. 1 Schematic diagram of test section

Chandra and Avedisian [9,10] presented photographs of heptane droplets impacting a heated surface. The relatively large (>1 mm) droplets at We=43 showed sensitivity to the surface temperature. At low temperature the droplets spread and evaporated while at higher temperature nucleate boiling was evident. Above the Leidenfrost temperature the droplets rebounded without any evidence of wetting.

Buyevich and Mankevich [11,12] modeled the impacted particles as liquid discs separated by a vapor layer whose thickness is that of the wall roughness. The liquid mass flux was assumed small enough to prevent formation of a liquid film on the heated surface. Based on the energy conservation of the droplet as well as the flow and heat conduction of the vapor interlayer between the droplet and wall, a critical impact velocity was identified to determine whether a droplet rebounds or is captured. Depending on their approach velocity, the impinging droplets are either reflected almost elastically or captured by the heated surface and completely vaporized within a sufficiently short time. They applied the model to dilute mist impingement with reported agreement with experiment.

Fujimoto and Hatta [13] studied deformation and rebound of a water droplet on a high-temperature wall. For Weber numbers of 10 to 60, they computed the distortions of the droplet as it flattened, contracted, and rebounded. They used a simple heat transfer model to confirm that surface tension dominates vapor production in the rebounding process. Hatta et al. [14] gave correlations of contact time and contact area of the droplet with Weber number.

Li et al. [15] presented an experimental study for 1.1 bar steam invested with water mist in a confined slot jet. Figure 1 is a schematic of the test article having a slot of width 7.5 mm located in a flat injection plate. The jet impacted a target wall of length 250 mm spaced 22.5 mm from the injection plate. The flow section had a width of 100 mm and Pyrex walls allowed vision of the heated surface. The droplet velocity and size distribution was obtained by a phase Doppler particle analyzer (PDPA). The experimental results are typified by Fig. 2. In the first panel the depression of temperature caused by mist is shown. Using the measured heat flux of Joulean heating in the wall divided by the wall to saturation temperature difference, the heat transfer coefficient of the second panel is produced. Panel three shows the enhancement, defined as the ratio of heat transfer coefficients with and without mist at the same Reynolds number. The cooling effect is signifi-

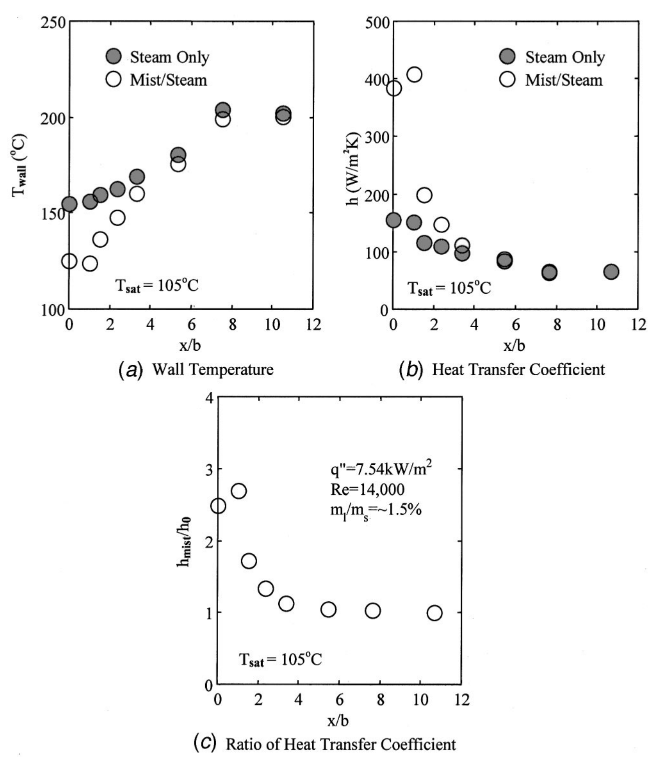

Fig. 2 A typical heat transfer result of mist/steam jet impingement (q''=7.54 kW/m^2, Re=14000, and m_l/m_s=~1.5 percent)

cant near the stagnation point and decreases to a negligible amount at 6 jet widths downstream. Up to 200 percent heat transfer enhancement at the stagnation point was achieved by injecting only ~1.5 percent by mass of mist. Direct observation through the Pyrex wall showed a dry heated surface in the experiment conditions, though no observations were made capable of disclosing the behavior of individual droplets in brief contact. The purpose of this communication is to model the processes of the experiment and trends with heat flux, mist concentration, and vapor velocity, based on Li et al. [15].

Basic Assumptions and Model

In mist/steam jet impingement, the droplets will not only influence the flow and temperature fields of the steam but also may interact directly with the target wall. In the experiment [15], water droplets, less than 15 μm diameter and at concentrations below 5 percent, impacted a heated surface with wall superheat below 60°C at a velocity up to 12 m/s. To model the heat transfer of the mist/steam impinging jet under these conditions, the following assumptions and approximations are made in this study:

- The wall is sufficiently heated to prevent accumulation of liquid.
- The interaction between droplets is ignored, since the average spacing between droplets is large.
- Because the droplet is small, no breakup is considered.
- The droplet is at the saturation temperature before entering the thermal boundary layer.
- The droplet has a less important effect on the velocity boundary layer than on the thermal boundary layer.

Under these assumptions, the heat transfer of mist/steam jet impingement is divided into three different parts: heat transfer from the target wall to the steam flow, heat transfer from the target wall to droplets and heat transfer between the steam and droplets. No radiative heat transfer is considered since the wall temperature is not very high in the current study and it is estimated to be less than 2 percent of the total heat transfer.

Heat Transfer From the Target Wall to the Steam. Heat transfer due to the steam is modeled as heat convection of a single-phase steam flow. Because of the disturbance by droplets on the boundary layer, this portion is subject to modification of the heat transfer coefficient of steam-only jet impingement flow. A detailed analysis of this effect must involve the effect of droplets on the flow field and the turbulence characteristics. The heat transfer enhancement through the effect of droplets on the flow has been assumed to be of secondary importance. Experimental study by Yoshida et al. [6] found 170 percent enhancement by adding 80 percent by mass glass beads of diameter 50 μm to the airflow. Considering the effect of the particles includes boundary layer disturbance as well as other cooling effects, the enhancement of the single-phase heat transfer due to droplets on the flow is projected to be less than 4 percent with a mist mass ratio of 2 percent.

Heat Transfer From the Target Wall to Droplets. Although many studies have been conducted on the interaction of the droplet with the bounding wall, few of these studies can be used to model the heat transfer from the target wall to droplets in the present study because of the different ranges of droplet size and flow parameters. Unlike spray cooling, where the droplet momentum is supplied by a device, small mist droplets may not be able to hit the wall because of the drag force in the present study. Based on trajectory analysis, it is believed that larger droplets will hit the wall if the approach velocity is high enough. Though neglected in trajectory analysis herein, the droplets are subject to the lift "force" of Ganic and Rosenhow [16] due to the momentum imbalance of asymmetric evaporation. A droplet in a temperature gradient near a heated wall is heated faster on the wall side. The difference in evaporation rate results in a lifting effect estimated to be of minor consequence for the conditions of this study.

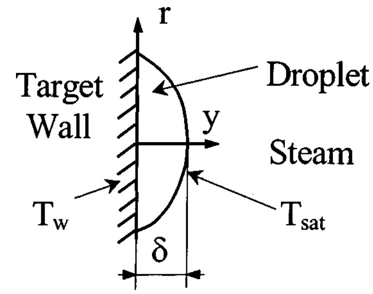

Fig. 3 Modeling of heat transfer from wall to droplet

The commercial code, FLUENT [17], a solver for the complete Navier Stokes equations using finite volume schemes, has been used to predict the trajectory of droplets including the determination of the impact velocity onto the heated surface. Complete details are included in Li [18] and only salient features are included here. The domain of Fig. 1 supplied with appropriate boundary conditions in the entrance and exit regions was subdivided to yield grid-independent results. The turbulent flow was modeled in several ways, with the k-ε model found to yield substantial agreement with the heat transfer results in single-phase steam flow. This computational model was combined with the dispersed-phase option of the program wherein droplets seeded in the entrance region of the flow were tracked and allowed both to affect the vapor flow and to evaporate in transit through the superheated layer. The droplets in the flow react with the fluid according to drag on a sphere at the slip velocity between the droplet and the fluid, usually very near the low velocity Stokes Flow asymptote.

Direct Contact Heat Transfer. According to Buyevich and Mankevich [11] (B&M model), the droplet will depart from the wall if the impact velocity is below a critical velocity, and stick if above. The critical velocity given by the B&M model is only about 0.6 m/s for $d=10\ \mu$m, $\Delta=0.5\ \mu$m and $T_w-T_{sat}=30°$C. This means that for the conditions of the current study most of the droplets will stick to the wall. According to the B&M model a sticking droplet will stay on the wall until evaporated completely. If most of the particles stick to the wall and evaporate completely the enhancement of heat transfer will be much higher than observed. Therefore the B&M model is found to be inadequate for this study.

The actual interaction between the droplets and wall is very complicated; it includes a continuous deformation of the droplet and is affected by droplet size and surface conditions. In this study, the heat transfer from wall to droplet is modeled simply by transient heat conduction to a spherical cap with a contact angle of 60 deg based on Gould [19] and Neumann et al. [20]. The corresponding height and base diameter of the cap are 0.464 and 1.608 times the original droplet diameter, respectively. Figure 3 shows the basic model $(\delta=0.464d)$. The configuration of the flattened droplet is assumed fixed until conditions for rebound are established.

Quasi-steady heat flow to a droplet has been considered by many authors including Sadhal and Martin [21] and Sadhal and Plesset [22]. Under some conditions exact solutions may be obtained. In the current work there is a need to include the transient warming of the droplet, as brief contact is anticipated. Since it is difficult to obtain an analytical solution, this problem is solved numerically by using FLUENT [17], with a non-uniform grid (r, y) of 50×50. Assuming a small fraction of the droplet evaporates before rebounding, a fixed-geometry (no allowance for the decrease of mass in evaporation) transient solution is sought with a uniform initial temperature of T_{sat}, the cap surface maintained at T_{sat}, and the base (wall) suddenly raised to T_w. Figure 4(a) shows the non-dimensional results for the total base heat flow Q

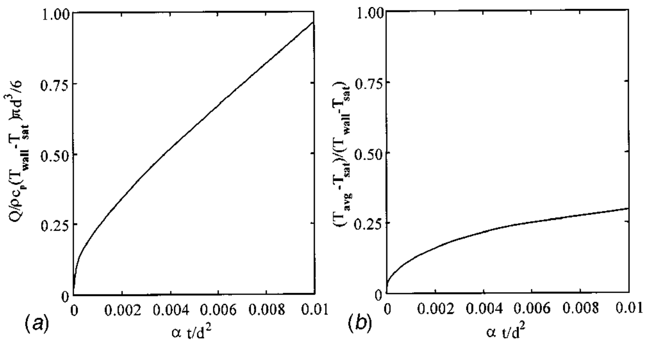

Fig. 4 Heat transfer process between droplet and wall by direct conduction (*Q* is the heat conduction from the target wall to the droplet): (*a*) total wall heat; and (*b*) superheat of droplet.

in terms of $\alpha t/d^2$. During contact the droplet is superheated in the amount given in Fig. 4(*b*). The heat entering the base and not residing in the droplet as superheat is conducted to the surface and is evaporated. There is no reference to the heat of vaporization because this quantity is not converted to a mass flow. The surface of the liquid maintained at the saturation temperature implies that the evaporative heat flux is included in the computation. For a temperature difference $(T_w-T_{\rm sat})$ of 30°C, the heat conduction in 1.2 μs evaporates 5 percent of a 5 μm droplet. Because the fraction of droplet evaporated is small, the assumption of constant domain size and shape yields a fast, yet reasonable result.

Residence Time on Target Surface. Once a droplet hits the wall, whether it rebounds from the wall depends on the wall temperature and impact velocity. The heat conduction model above cannot give the essential condition for rebounding. To complete this model, the residence time of the droplet on the wall must be determined. It is conceivable that the droplets may wet the surface and stick on the heated wall until a vapor layer forms from nucleation at the base. Upon formation of this layer the droplet would return to its spheroidal shape and depart. A concept in pool boiling has a waiting time during which the region near the wall becomes superheated to the point where nucleation becomes spontaneous. Based on nucleation in a small cavity on the heated surface, Mikic and Rohsenow [23] studied the waiting time and provided the following simple estimate:

$$t_w=\frac{1}{\pi\alpha}\left\{\frac{(T_w-T_{\rm sat})r_c}{T_w-T_{\rm sat}(1+2\sigma/\rho_g H_{fg} r_c)}\right\}^2. \tag{1}$$

Here r_c is the radius of the nucleation cavity. This equation gives a waiting time of about 11 μs with $r_c=2\ \mu$m and $T_w-T_{\rm sat}=30$°C. The principal attractive feature of this concept is that the waiting time decreases slightly as the wall temperature increases. Because this waiting time depends strongly on the value of r_c that is difficult to determine, this model cannot be applied confidently for the present study. Besides, this model does not account for the effects of the droplet size and impact velocity.

Although the impact velocity was considered, the scale of the residence time given by Hatta et al. [14] did not include any wall temperature effect. The reason may be that their experiment was conducted at a very high wall temperature (above the Leidenfrost temperature). If the wall temperature is low, the free-slip boundary condition used in their study cannot be used any more. This basis for time scale will give a constant cooling enhancement for all wall temperatures, which is not the case from experiments. The Hatta model is expected to be valid as the temperature rises; it should from a lower bound for the contact time.

For our selected model it is assumed that the droplet will deform into the lens shape of Fig. 3 and remain on the wall momentarily without wetting gaining superheat according to the transient process of heat conduction discussed already. A vapor layer will form in response to the superheat until it reaches a sufficient pressure to repel the droplet. We reason that the pressure must overcome surface deformation (expressed through σ/d) and supply an exit velocity (pressure expressed through We σ/d) proportional to the entering velocity of impact. The temperature required to provide this pressure is that associated by the slope of the liquid-vapor saturation curve, wherein the required pressure is translated to a required superheat. Finally the superheat is linearly related to the product of wall superheat and the residence time. Expressed non-dimensionally, there results

$$\frac{\alpha t_r}{d^2}=\frac{c}{T_w-T_{\rm sat}}\left.\frac{dT}{dP}\right|_{\rm sat}\left[\frac{\sigma}{d}(1+{\rm We}/8)\right]. \tag{2}$$

Here the constant, c, which depends on the geometry selected for the heat conduction model, is found by trial and error to be about 4.8×10^{-2} to agree with the experiment. The effect of impact velocity is not strong if the Weber number is small. This residence time is actually an effective value because it simplifies the deformation process of the droplet on the wall. The residence time of a 10 μm droplet with a Weber number of 1 and a temperature difference of 30°C is 1.7 μs. This model is expected to fail at high wall temperature where the residence time goes to zero. In this case, however, it is believed that the droplet will still contact the wall for at least the lower bound established by the deformation process.

Heat Transfer Between the Droplet and Steam. Heat transfer between the droplets and steam can be modeled by considering droplets as a distributed heat sink. The droplets evaporate into the superheated steam inside the thermal boundary layer and act to quench the boundary layer. Based on the superposition concept the temperature of mist/steam flow is divided into two parts, $T=T_1+T_2$. $T_1(x,y)$ is the temperature of steam-only flow and $T_2(y)$ is the temperature depression caused by the mist.

The two-dimensional energy equation with a distributed heat sink is given as

$$\rho c_p u\frac{\partial T}{\partial x}+\rho c_p v\frac{\partial T}{\partial y}=k_s\frac{\partial^2 T}{\partial x^2}+k_s\frac{\partial^2 T}{\partial y^2}-k_s\beta^2(T-T_{\rm sat}). \tag{3}$$

The last term is a heat sink per unit volume to a distributed surface at temperature $T_{\rm sat}$. The coefficient, β, is equal to $(12c_{\rm mist}\rho_s d_{10}/\rho_1 d_{30}^3)^{0.5}$ and $c_{\rm mist}$ is the mist concentration. $k_s\beta^2$ is the hA of the droplets per unit volume with $hd/k_s=2$ and $k_s\beta^2(T-T_{\rm sat})$ is the heat sink per volume. $hd/k_s=2$ is chosen for slip Re$\ll$1 for most droplets in the current study.

The equation for T_1 can be written as

$$\rho c_p u\frac{\partial T_1}{\partial x}+\rho c_p v\frac{\partial T_1}{\partial y}=k_s\frac{\partial T_1}{\partial x^2}+k_s\frac{\partial^2 T_1}{\partial y^2}. \tag{4}$$

For the current study, the boundary conditions for T_1 include $\partial T_1/\partial x=0$ at $x=0$ and $x=L/2$ and for y

$$T_1=T_w \quad \text{at} \quad y=0 \tag{5a}$$

$$T_1=T_{\rm sat} \quad \text{at} \quad y\rightarrow\infty. \tag{5b}$$

Solution for Eq. (4) subject to (5) together with flow descriptions will produce a result for pure steam. In this work no solution is presented; rather the result is known from experiment to produce $h_0(x)=q''/(T_w-T_{\rm sat})$. In [15] the experimental result is shown to agree substantially with other investigations. In lieu of an analytical solution, the following near-wall temperature distribution is assumed.

$$T_1=(T_w-T_{\rm sat})e^{-yh_0/k_s}+T_{\rm sat}, \tag{6}$$

where h_0 is the heat transfer coefficient obtained from experimental study. T_w and h_0 depend on *x*.

Considering T_2 is a function of *y* only, the equation for T_2 can be simplified as

$$k_s \frac{d^2 T_2}{dy^2} - \rho c_p v \frac{dT_2}{dy} - k_s \beta^2 (T_1 + T_2 - T_{\text{sat}}) = 0. \tag{7}$$

The boundary conditions for Eq. (7) are

$$T_2 = 0 \quad \text{at} \quad y = 0 \quad \text{and} \quad y \to \infty. \tag{8}$$

This equation is first solved without considering the second term and the result for $\beta \neq h_0/k_s$ can be given as

$$T_2 = \frac{\beta^2 (T_w - T_{\text{sat}})}{\beta^2 - (h_0/k_s)^2} (e^{-\beta y} - e^{-y h_0/k_s}). \tag{9}$$

Therefore, the heat transfer augmentation due to mist, h_2, defined as $-k_s(dT_2/dy)|_{y=0}/(T_w - T_{\text{sat}})$, can be given by

$$\frac{h_2}{h_0} = \frac{(\beta k_s/h_0)^2}{\beta k_s/h_0 + 1}. \tag{10}$$

Assume that $h_0 = 100\,\text{W/m}^2\text{K}$, $c_{\text{mist}} = 2$ percent and $d_{10}/d_{30}^3 = 10^{10}\,\text{m}^{-2}$, a value of $h_2/h_0 = 0.069$ is obtained. A value for c_{mist} of 10 percent will give a value of 0.269 for h_2/h_0.

The effect of the second term, $\rho_s c_p v \, dT_2/dy$ can be evaluated using Eq. (9). The velocity, v, leaving the boundary layer is estimated to be only about 0.25 mm/s by integrating the vapor generated from droplet evaporation. For the conditions of the example, this results in a value of the second term about 1 percent of the sink term and is neglected. The solution for T_2 given by Eq. (9) is accepted as an approximation.

The liquid concentration near the target wall might be different from the average concentration because the droplets cross the streamlines. However, migration of the droplets away from the wall occurs due to the lift forces and turbulent dispersion makes the mist concentration more uniform and close to the average value. Therefore, the quenching effect of the mist is estimated with the average concentration. Surveys by PDPA support this assumption.

Model Validation

The average heat transfer within $x/b < 1$ is considered. As an example, a distribution of droplet size from the experimental study is given in Fig. 5(*a*) at the jet exit for Re=14,000 and $m_l/m_s = 1.5$ percent. This size distribution, obtained by PDPA measurement entering the test section, gives the average diameters of $d_{10} = 4.7\,\mu$m and $d_{30} = 6.4\,\mu$m. By using FLUENT [17], the droplet distribution impacting the wall is given in Fig. 5(*b*). For the case cited, it is predicted that droplets less than 5 μm will not impact the wall, which means there is no direct heat conduction from the wall to droplets. The heat transfer to small droplets is mainly through the steam. Though not shown there is divergence of the pathlines resulting in diminished droplet flux at the stagnation point. The impact velocity varies with droplet size and injection location and for the case cited it ranges up to 12 m/s.

Table 1 lists five different cases to be predicted. Case 1 is the case shown in Fig. 2. The predicted results are given in Table 2. The input to the analytical model includes h_0, T_w, T_{sat}, m_l/m_s, as well as the droplet size distribution by PDPA. In Table 2, $q_1'' = h_0(T_w - T_{\text{sat}})$ is the single-phase heat transfer from wall to steam, q_2'' using Eq. (10) is the quenching effect of the mist; and q_3'' is the direct heat conduction during the contact time of Eq. (2) from wall to droplet. It can be seen that the predicted results and the experimental data have good agreement, especially when considering the experimental uncertainty. The relative size of the various contributions is shown clearly in Table 2 and q''_{exp}/q''_1 is the heat transfer enhancement ratio, h_{mist}/h_0. The q_3'' component dominates q_2''. Both q_2'' and q_3'' become important in proportion to mist concentration.

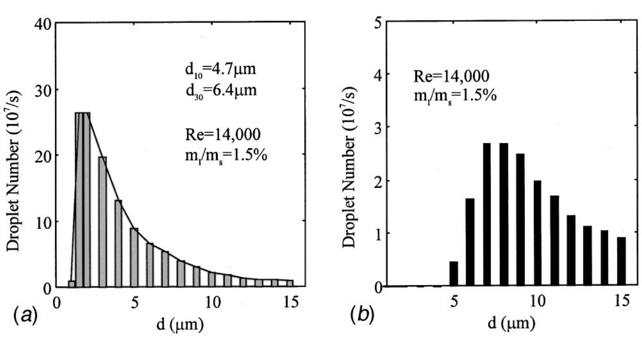

Fig. 5 Droplet distribution and number at jet exit and on target wall: (*a*) at jet exit; and (*b*) impacting on target wall ($x/b < 1$).

Table 1 Experimental cases

Case	Re	h_0 (W/m²K)	T_w (°C)	T_{jet} (°C)	m_l/m_s (%)	q'' (W/m²)	h/h_0
1	14,000	150	125	105	1.5	7,540	2.5
2	22,500	210	130	105	1.75	20,900	4.0
3	22,500	210	165	105	0.75	20,900	1.7
4	7,500	105	138	103	3.5	7,540	2.1
5	14,000	153	154	105	1.5	13,400	1.8

Table 2 Results of the model

Case	Prediction Results (W/m²)				q''_{exp} (W/m²)	Error (%)
	q_1''	q_2''	q_3''	q''_{total}		
1	3,000	131	4,143	7,274	7,540	-3.5
2	5,250	143	15,196	20,589	20,900	-1.5
3	12,600	149	8,504	21,253	20,900	1.7
4	3,675	627	2,746	7,048	7,540	-6.5
5	7,497	317	5,691	13,505	13,400	0.8

Prediction of Parametric Effects

The general aim of the prediction is to determine the heat transfer due to droplet injection, given wall temperature, Reynolds number, liquid concentration and droplet distribution. Firstly, the analytical model discussed above requires the droplet size distribution. Secondly, the impinging velocity and deposition rate on the heated surface must be known. These can be evaluated respectively by empirical equations or obtained by numerical simulation. Thirdly, determine the heat removal from the target wall directly by the droplets. Lastly, add the heat transfer by the two other components and obtain the total heat transfer.

The current analytical model can successfully predict the effect of various parameters observed in the experiment. When the wall temperature increases, the heat transfer from wall to steam and from steam to droplets will increase proportionally with the temperature difference. However, the heat transfer due to the direct conduction from wall to droplets will change little (compare cases 1 and 5) because the residence time becomes short. Therefore, the ratio of heat transfer coefficients will decrease, which has been observed in experimental studies. Figure 6 shows the predicted result of the wall temperature effect, given the mist concentration and impact velocity for 10 μm droplets and a single-phase heat transfer coefficient of 150 W/m²-K. As shown in this figure, the droplet impact velocity is an important variable affecting droplet heat transfer, a trend in agreement with the experiment by Pederson [9]. Figure 7 shows the comparison of the model result and the experimental data. Here the droplet size distribution measured

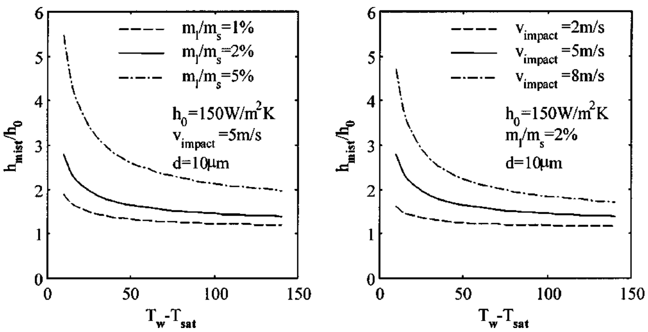

Fig. 6 Predicted effect of the wall temperature on mist/steam heat transfer at different mist concentrations and droplet impact velocities

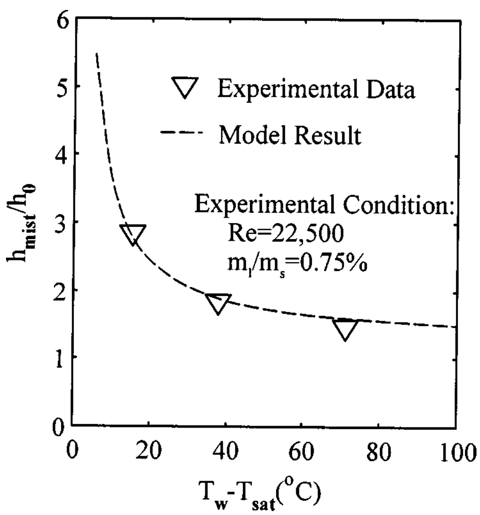

Fig. 7 Comparison of the predicted result by the model and experimental data

from experiment is used; impact density and velocity have been predicted by FLUENT's dispersed flow feature. The agreement is substantial.

Figure 8 shows the predicted trend of enhancement with mist concentration, given the wall temperature, droplet size and impact velocity. The same single-phase heat transfer coefficient as in Fig. 6 is used. The enhancement of heat transfer is proportional to the mist concentration. With a fixed value of impact velocity, smaller droplets provide greater enhancement. However, this result cannot be used simplistically because the impact velocity of a droplet depends on the jet velocity as well as the droplet size. Small droplets always have a small impact velocity if they have enough momentum to reach the wall.

Given wall temperature and mist concentration, if the jet velocity increases, the heat transfer from wall to steam will increase but the heat transfer from steam to droplet will decrease due to the thinner boundary layer (see Eq. (10)). The heat transfer from wall to droplet will increase as more droplets hit the wall at higher impact velocity. As a result, the overall heat transfer enhancement increases when the jet velocity increases. This tendency is verified by experiment.

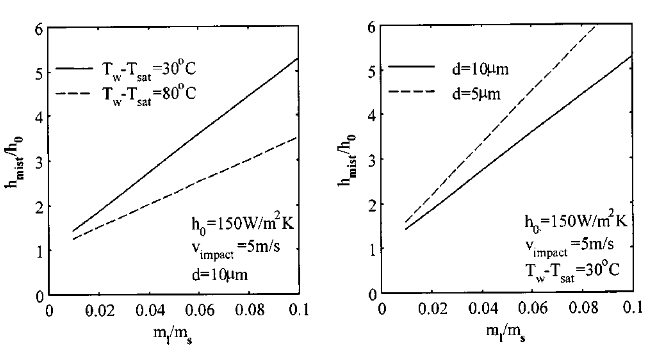

Fig. 8 Predicted effect of the mist concentration on mist/steam heat transfer at different wall temperatures and droplet diameter

Conclusions

A model for mist/steam jet cooling has been developed and presented which considers the total heat flow to be comprised of three components. A single-phase-like heat flow and a boundary layer quenching effect account for heat flow leaving the surface through the steam. To this is added a heat flow occurring in brief contacts with impacting droplets.

Heat conduction from the wall to droplets is found to be the dominant enhancement mechanism. The quenching effect of droplets in the steam flow becomes important when the mist concentration is high. The heat transfer to small droplets is mainly through the steam while larger droplets hit and cool the heated wall by direct heat conduction.

Because the enhancement increases at lower wall temperature, the contact time for direct conduction varies inversely with wall superheat. A contact time correlation is proposed which, with a simple conduction model, accounts for the observed heat transfer within the experimental uncertainty. The model depends on size distribution, impact velocity and density for droplets, requiring a dispersed-phase trajectory model.

All mechanisms of cooling are proportional to mist concentration. The effect of vapor velocity is mildly positive on the enhancement. The effect of droplet size has both positive and negative components and the model has implied predictions but these are not known from experiment.

Acknowledgments

The authors would like to thank Graver Separations (Wilmington, DE) for donating the steam filters for the experiment. We also want to thank Mee Industries Inc. (El Monte, CA) for donating the pressure atomizers and the high pressure pump. We appreciate the help from Dr. T. Guo in setting up the test facility. This research was sponsored by the U.S. Department of Energy under the contract DOE/AGTSR 95-01-SR-034, and was managed by Dr. N. Holcombe at the Federal Energy Technology Center and by Dr. Larry Golan at the South Carolina Institute for Energy Studies.

Nomenclature

A = area (m^2)
b = jet width (7.5 mm)
c = mass concentration
c_p = specific heat capacity (J/kg-K)
d = diameter of droplet (μm)
d_{10} = arithmetic mean diameter (μm)
d_{30} = volume mean diameter (μm)
d_{32} = Sauter mean diameter (μm)
H_{fg} = latent heat (J/kg)
h = heat transfer coefficient$=q''/(T_w-T_{sat}$ (W/m^2-K)
h_{mist} = heat transfer coefficient of mist (W/m^2-K)
h_0 = steam-alone heat transfer coefficient (W/m^2-K)
k = heat conductivity (W/m-K)
m = mass flow rate (kg/s)
P = pressure (N/m^2)
Q = heat conduction$=\int_0^{t} q'' A dt (J)$
q'' = heat flux (W/m^2)
Re = Reynolds number ($\rho_s v_j 2b/\mu_s$)

r = coordinate in the radial direction (m)
T = temperature (K)
t = time (s)
t_r = residence time (s)
y, v = velocity components in x, y directions (m/s)
v_j = jet velocity (m/s)
We = Weber number ($\rho v^2 d/\sigma$)
x = coordinate along the target wall (m)
y = coordinate perpendicular to the target wall (m)
α = thermal diffusivity (m^2/s)
β = variable defined in Eq. (3)
Δ = thickness of vapor layer (m)
δ = height of spherical cap (m)
μ = dynamic viscosity (kg/m-s)
ρ = density (kg/m^3)
σ = surface tension (N/m)

Subscripts

l = liquid phase
s = steam
sat = saturated
w = wall

References

[1] Goodyer, M. J., and Waterston, R. M., 1973, ''Mist-Cooled Turbines,'' *Conf. of Heat and Fluid Flow in Steam and Gas Turbine Plant*, Proc. of Institution of Mechanical Engineers, pp. 166–174.
[2] Guo, T., Wang, T., and Gaddis, J. L., 2000, ''Mist/Steam Cooling in a Heated Horizontal Tube Part I: Experimental System and Part II: Results and Modeling,'' ASME J. Turbomach., **122**, pp. 360–374.
[3] Guo, T., Wang, T., and Gaddis, J. L., 2000, ''Mist/Steam Cooling in a 180-Degree Tube,'' ASME J. Heat Transfer, **122**, No. 4, pp. 749–756.
[4] Takagi, T., and Ogasawara, M., 1974, ''Some Characteristics of Heat and Mass Transfer in Binary Mist Flow,'' *Proc. of 5th Int. Heat Transfer Conf.*, Tokyo, Japan Society of Mechanical Engineers, pp. 350–354.
[5] Mastanaiah, K., and Ganic, E. N., 1981, ''Heat Transfer in Two-Component Dispersed Flow,'' ASME J. Heat Transfer, **103**, pp. 300–306.
[6] Yoshida, H., Suenaga, K., and Echigo, R., 1988, ''Turbulence Structure and Heat Transfer of A Two-Dimensional Impinging Jet with Gas-Solid Suspensions,'' NHTC, **2**, pp. 461–467.
[7] Wachters, L. H. J., Smulders, L., Vermeulen, J. R., and Kleiweg, H. C., 1966, ''The Heat Transfer from A Hot Wall to Impinging Mist Droplets in The Spheroidal State,'' Chem. Eng. Sci., **2**, pp. 1231–1238.
[8] Pederson, C. O., 1970, ''An Experimental Study of the Dynamic Behavior and Heat Transfer Characteristics of Water Droplet Impinging upon a Heated Surface,'' Int. J. Heat Mass Transf., **13**, pp. 369–381.
[9] Chandra, S., and Avedisian, C. T., 1992, ''Observations of Droplet Impingement on a Ceramic Porous Surface,'' Int. J. Heat Mass Transf., **35**, No. 10, pp. 2377–2388.
[10] Chandra, S., and Avedisian, C. T., 1991, ''On the Collision of a Droplet With a Solid Surface,'' Proc. R. Soc. London, Ser. A, **432**, pp. 13–41.
[11] Buyevich, Yu. A., and Mankevich, V. N., 1995, ''Interaction of Dilute Mist Flow with a Hot Body,'' Int. J. Heat Mass Transf., **38**, pp. 731–744.
[12] Buyevich, Yu. A., and Mankevich, V. N., 1996, ''Cooling of a Superheated Surface with a Jet Mist Flow,'' Int. J. Heat Mass Transf., **39**, pp. 2353–2362.
[13] Fujimoto, H., and Hatta, N., 1996, ''Deformation and Rebounding Processes of a Water Droplet Impinging on a Flat Surface above Leidenfrost Temperature,'' ASME J. Fluids Eng., **118**, pp. 142–149.
[14] Hatta, N., Fujimoto, H., Kinoshita, K., and Takuda, H., 1997, ''Experimental Study of Deformation Mechanism of a Water Droplet Impinging on Hot Metallic Surfaces above Leidenfrost Temperature,'' ASME J. Fluids Eng., **119**, pp. 692–199.
[15] Li, X., Gaddis, J. L., and Wang, T., 2001, ''Mist/Steam Heat Transfer in Confined Slot Jet Impingement,'' ASME J. Turbomach., **123**, No. 1, pp. 161–167.
[16] Ganic, E. N., and Rosenhow, W. M., 1977, ''Dispersed Flow Heat Transfer,'' Int. J. Heat Mass Transf., **20**, pp. 885–866.
[17] Fluent, 1997, FLUENT 4.4 User's Guide, I–III, Fluent Inc.
[18] Li, X., 1999, ''Cooling by a Mist/Steam Jet,'' Ph.D. dissertation, Dept. of Mechanical Engineering, Clemson University, SC.
[19] Gould, R. F., 1964, *Contact Angle, Wettability and Adhesion*, American Chemistry Society, DC.
[20] Neumann, A. W., and Spelt, J. K., 1996, *Applied Surface Thermodynamics*, Marcel Dekker, Inc., NY.
[21] Sadhal, S. S., and Martin, W. W., 1977, ''Heat Transfer Through Drop Condensate Using Differential Inequalities,'' Int. J. Heat Mass Transf., **20**, No. 12, pp. 1401–1407.
[22] Sadhal, S. S., and Plesset, M. S., 1979, ''Effect of Solid Properties and Contact Angle in Dropwise Condensation and Evaporation,'' ASME J. Heat Transfer, **101**, No. 1, pp. 48–54.
[23] Mikic, B. B., and Rohsenow, W. M., 1969, ''Bubble Growth Rates in Non-Uniform Temperature Field,'' Prog. Heat Mass Transfer, **2**, pp. 283–292.